Production of vector bosons in association with jets in CMS

Meena Meena[a,b]
[a] *Panjab University,*
Chandigarh, India
[b] *On behalf of the CMS Collaborations*
E-mail: meena.meena@cern.ch/meenaluhach91@gmail.com

The study of the associated production of vector bosons and jets constitutes an excellent environment to check numerous Quantum Chromodynamics predictions and help to improve the understanding of the proton structure. Total and differential cross sections of vector bosons produced in association with heavy quarks and jets have been studied in proton-proton collisions using CMS data. Differential distributions as function of a broad range of kinematic observables are measured and compared with several theoretical predictions.

1. Introduction

In this paper, recent results are presented on vector boson and heavy flavor (HF) production obtained using proton-proton (pp) collision data collected by the CMS Experiment [1] at the Large Hadron Collider (LHC).

2. Measurement of associated production of a W boson and a charm (c) quark at the center-of-mass energy ($\sqrt{s}$) = 13 TeV

The differential and integrated cross section measurements of W and c quark production are performed using data collected by the CMS Experiment in 2016 corresponding to an integrated luminosity (L) of 35.7 fb^{-1} [2]. The associated production of W bosons and c quarks in pp collisions at the LHC probes the strange (s) quark content of the proton directly through the leading order (LO) processes $\mathrm{g} + \bar{\mathrm{s}} \rightarrow \mathrm{W}^{+} + \bar{\mathrm{c}}$ and $\mathrm{g} + \mathrm{s} \rightarrow \mathrm{W}^{-} + \mathrm{c}$. Only a few percent of the total cross section is contributed by the processes $\mathrm{g} + \bar{\mathrm{d}} \rightarrow \mathrm{W}^{+} + \bar{\mathrm{c}}$ and $\mathrm{g} + \mathrm{d} \rightarrow \mathrm{W}^{-} + \mathrm{c}$. Therefore, measurements of associated W + c production in pp collisions provide useful information about the s quark distribution of the proton. The parton distribution functions (PDFs) are used to describe the structure of the proton, and PDFs are determined by comparing theoretical predictions obtained at a particular order in perturbative quantum chromodynamics (pQCD) to experimental measurements. The precision of the PDFs, which affects the accuracy of the theoretical predictions for cross sections at the LHC, is determined by using the uncertainties of the experimental measurements, and by the limitations of the available theoretical calculations.

In this measurement, W bosons are identified by their decay into a muon (μ) and a neutrino. The presence of a neutrino in an event is assured by imposing a requirement on the transverse mass (m_{T}), which is defined as the combination of muon transverse momentum (p_{T}^{μ}) and missing transverse momentum ($\overrightarrow{p_{\mathrm{T}}}^{\mathrm{miss}}$):

$$m_{\mathrm{T}} = \sqrt{2 p_{\mathrm{T}}^{\mu} \overrightarrow{p_{\mathrm{T}}}^{\mathrm{miss}} (1 - \cos(\phi_{\mu} - \phi_{\overrightarrow{p_{\mathrm{T}}}^{\mathrm{miss}}}))}.$$

The dominant background originates from processes like $\mathrm{u} + \bar{\mathrm{d}} \rightarrow \mathrm{W}^{+} + \mathrm{g}^{*} \rightarrow \mathrm{W}^{+} + \mathrm{c}\bar{\mathrm{c}}$ or $\mathrm{d} + \bar{\mathrm{u}} \rightarrow \mathrm{W}^{-} + \mathrm{g}^{*} \rightarrow \mathrm{W}^{-} + \mathrm{c}\bar{\mathrm{c}}$, with c quarks produced in gluon splitting. In the W + c signal events, the charges of the W boson and the c quark have opposite signs (OS). In gluon splitting, an additional c quark is produced with the same charge as the W boson (SS).

The c quarks are tagged by a full reconstruction of the charmed hadrons in the process $\mathrm{c} \rightarrow \mathrm{D}^{*}(2010)^{\pm} \rightarrow \mathrm{D}^{0}(1896) + \pi^{\pm}_{slow} \rightarrow K^{\mp} + \pi^{\pm} + \pi^{\pm}_{slow}$. The signal is extracted from the Δm distribution, i.e. $m(K\pi\pi) - m(K\pi)$, in which resolution effects from the D^{0} reconstruction cancel, leading to a narrow D^{*} signal. A cross section is measured in the fiducial region defined by $p_{\mathrm{T}}^{\mu} >$ 26 GeV, $|\eta^{\mu}| < 2.4$, $m_{\mathrm{T}} \geq 50$ GeV, and $p_{\mathrm{T}}^{\mathrm{c}} > 5$ GeV. An event is selected as a W + c signal if it contains a W + $\mathrm{D}^{*}(2010)^{\pm}$ and the background contributions from gluon splitting are removed by subtracting the SS events from the OS events. The contributions from other background sources, such as $\mathrm{t}\bar{\mathrm{t}}$ and single top quark production, are negligible. The inclusive cross section and cross section ratio are $\sigma(\mathrm{W} + \mathrm{c}) = 1026 \pm 31\ (\mathrm{stat})^{+76}_{-72}\ (\mathrm{syst})$ pb and $\sigma(\mathrm{W}^{+} + \bar{\mathrm{c}})/\sigma(\mathrm{W}^{-} + \mathrm{c}) = 0.968 \pm 0.055\ (\mathrm{stat})^{+0.015}_{-0.028}\ (\mathrm{syst})$, respectively. The measurements are compared to the next-to-leading order

(NLO) predictions calculated using the ABMP16nlo [3], ATLASepWZ16nnlo [4], CT14nlo [5], MMHT14nlo [6], NNPDF3.0nlo [7], and NNPDF3.1nlo [8] PDF sets. Good agreement is observed between the measured W + c cross section and NLO calculations except for the prediction using the ATLASepWZ16nnlo PDF set as shown in Figure 1 (left). For the cross section ratio $\sigma(\mathrm{W}^+ + \bar{\mathrm{c}})/\sigma(\mathrm{W}^- + \mathrm{c})$, all theoretical predictions are in good agreement with the measured value.

The present measurement probes the s quark distribution directly in the kinematic range of $\langle x\rangle \approx 0.007$ at the scale of m_{W}^2, where x is the Bjorken scaling variable. To illustrate the impact of this measurement in the determination of the s quark distribution in the proton, the data is used in a QCD analysis at NLO together with inclusive deep inelastic scattering (DIS) measurements [9] and earlier results from CMS on W + c production at $\sqrt{s}$ = 7 TeV [10] and available CMS measurements of the lepton charge asymmetry in W boson production at $\sqrt{s}$ = 7 TeV [11] and at $\sqrt{s}$ = 8 TeV [12]. The procedure for the determination of the PDFs follows the approach used in the earlier CMS analyses [11]–[12]. The s quark distribution is determined by fitting the free parameters. For all measured data, the predicted and measured cross sections together with their corresponding uncertainties are used to build a global χ^2, minimized to determine the initial PDF parameters [13]–[14]. Also, a partial χ^2 divided by the number of measurements (data points), is provided. The global and partial χ^2 values show a general agreement among all the data sets. The s quark distribution $\mathrm{s}(\mathrm{x}, \mathrm{Q}^2)$ and the strangeness suppression factor $\mathrm{r_s}(\mathrm{x}, \mu_f^2) = (\mathrm{s} + \bar{\mathrm{s}})/(\bar{\mathrm{u}} + \bar{\mathrm{d}})$ are determined at the factorization scale (μ_f^2) of 1.9 GeV^2 and m_{W}^2 and agree with earlier results obtained in neutrino scattering experiments [15]-[18]. The s quark distribution is shown in Figure 1 (middle). Despite differences in the data used in the individual global PDF fits, the $\mathrm{r_s}$ distributions in ABMP16nlo, NNPDF3.1nlo, CT14nlo, and MMHT14nlo are in a good agreement among each other and disagree with the ATLASepWZ16nnlo result [4]. The ABMP16nlo PDF includes the most recent data on c quark production in charged-current neutrino-nucleon DIS collected by the NOMAD and CHORUS experiments in order to improve the constraints on the s quark distribution and to perform a detailed study of the isospin asymmetry of the light quarks in the proton sea. In Figure 1 (right), the $\mathrm{r_s}$ is shown in comparison with the ATLASepWZ16nnlo and the ABMP16nlo. Whereas the CMS result for $\mathrm{r_s}(\mathrm{x})$ is close to the ABMP16nlo PDF, it shows a significant difference with regard to the ATLASepWZ16nnlo PDF for $\mathrm{x} > 10^{-3}$. The significant excess of the s quark content in the proton reported by ATLAS is not observed in the present analysis.

3. Measurement of the Z + HF jets cross section at the $\sqrt{s}$ of 13 TeV

The differential and integrated cross section measurements of $\mathrm{Z}(\rightarrow ll) + \geq 1$ c jet [19], where $ll = e^+e^-$ or $\mu^-\mu^+$ and cross section ratios of the Z + b jet and Z + c jet w.r.t Z + jet (R(b/j), R(c/j)), and Z + c jet w.r.t Z + b jet (R(c/b)) [20] are performed using the data collected in 2016 corresponding to L of 35.9 fb^{-1}. The differential and integrated cross section measurements of Z + $\geq$ 1 b jet, Z + $\geq$ 2 b jets, and cross section ratio of the Z + $\geq$ 2 b jets w.r.t Z + $\geq$ 1 b jet are performed using data collected during 2016–2018 corresponding to L of 137 fb^{-1} [21].

The b jets or c jets are those jets that are initiated by b or c quarks with a characteristic lifetime of $\sim$ 1.5 (1.1) ps of the b (c) hadron. The b (c) hadron travels $\approx$1 cm at energy $\approx$ 10–100 GeV in the laboratory frame before decaying to several particles and forming a new vertex called the secondary vertex. The invariant mass and impact parameter of the tracks associated with this secondary vertex

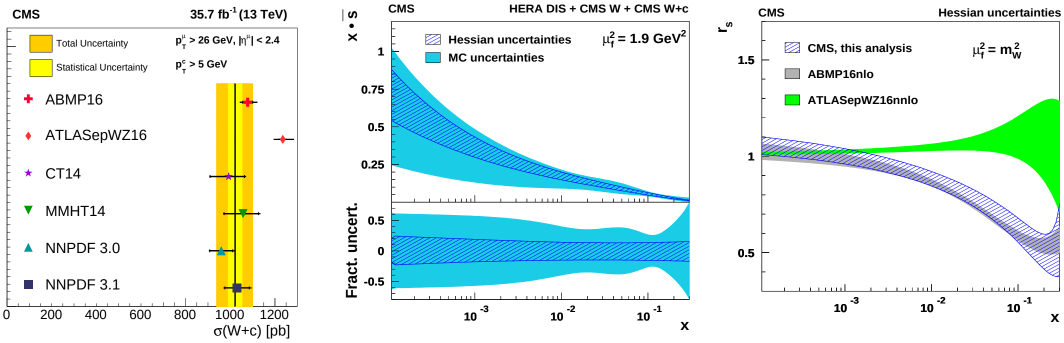

Figure 1: Inclusive fiducial cross section $\sigma(\mathrm{W+c})$ at 13 TeV (left). The s quark distribution as a function of x at the μ_f^2 of 1.9 GeV^2. The results of the current analysis are presented with the fit uncertainties estimated by the Hessian method (hatched band) and using MC replicas (shaded band) (middle). The r_s as a function of x at the μ_f^2 of m_W^2 of the current analysis (hatched band) are compared to ABMP16nlo (dark shaded band) and ATLASepWZ16nnlo (light shaded band) PDFs (right) [2].

are the input variables to the b-tagging/c-tagging Deep Combined Secondary Vertices algorithm DeepCSV [22]. This algorithm discriminates between signal and background. In the Z + ≥ 1 c jets and Z + HF jets cross section ratio analyses, the secondary vertex mass (M_{SV}) is used to correct simulation by applying the corresponding scale factors for the Z + c jet, Z + b jet, and Z + light jet components. These scale factors are obtained by fitting M_{SV} templates from simulation to the observed data. Figure 2 (left) shows the distribution of M_{SV} after applying the scale factor and there is good agreement between the data and the simulation.

The fiducial phase space regions is defined as follows. The Z boson candidate is reconstructed by requiring a pair of oppositely charged two electrons or two muons within the mass range of 71 and 111 GeV and $|\eta| < 2.4$. The Z boson candidate is required to be accompanied by at least one inclusive or b jet or c jet selected with $p_T > 30$ GeV and $|\eta| < 2.4$.

Due to detector resolution and the event selection inefficiency, there can be migrations between bins of reconstructed distributions and it can alter the true distributions. Therefore, bin-by-bin migrations are corrected by the response matrices, which describe the migration probability between the particle- and reconstructed-level quantities of a given observable (for example Z or jet p_T).

The total fiducial measured cross section of the Z + c jet to be 405.4 ± 5.6 (stat) ± 24.3 (exp) ± 3.7 (theo) pb. The differential cross sections for inclusive Z + c jet production as a function of c jet p_T are shown in Figure 2 (middle). The measured integrated cross section ratio values are R(c/j) = 0.102 ± 0.002 (stat) ± 0.009 (syst), R(b/j) = 0.0633 ± 0.0004 (stat) ± 0.0015 (syst), and R(c/b) = 1.62 ± 0.03 (stat) ± 0.15 (syst). The differential cross section ratios of R(c/b) as a function of jet p_T are shown in Figure 2 (right). The measured integrated cross sections for the Z + ≥ 1 b jet and Z + ≥ 2 b jets are 6.52 ± 0.04 (stat) ± 0.40 (exp) ± 0.14 (th) pb and 0.65 ± 0.03 (stat) ± 0.07 (exp) ± 0.02 (th) pb, respectively. The measured integrated cross section ratio of the Z + ≥ 2 b jets to Z + ≥ 1 b jet is 0.100 ± 0.005 (stat) ± 0.007 (exp) ± 0.003 (th) pb. The differential cross section distributions for the Z + ≥ 1 b jet, Z + ≥ 2 b jets and cross section ratio of Z + ≥ 2 b jets to Z + ≥ 1 b jet as a function of leading b jet p_T are shown in Figure 2 (left), (middle), and (right), respectively. The predictions for Z + b and Z + c jet production can be derived in either a

4-flavor number scheme (4FNS) or a 5-flavor number scheme (5FNS). In 5FNS, b quark density is allowed in the initial state via a b quark PDFs of proton but not in 4FNS. The measured integrated cross sections of the Z + c jet, R(c/j), R(b/j), Z + ≥ 1 b jet, and Z + ≥ 2 b jets are overestimated by MG5_aMC NLO 5FNS, except R(c/b). The Z + c jet, R(c/j), R(b/j), Z + ≥ 1 b jet, and Z + ≥ 2 b jets are well described by the MG5_aMC LO 5FNS. The SHERPA NLO 5FN simulation overestimates the measured integrated cross sections of the Z + c jet, Z + ≥ 1 b jet, and Z + ≥ 2 b jets; however, it provides a good description of the shapes of various kinematic observables. The R(c/j) and R(c/b) are underestimated and R(b/j) is overestimated by the MCFM predictions at LO and NLO. The measured value of the cross section ratio Z + ≥ 2 b jets/Z + ≥ 1 b jet is well described by the MG5_aMC (LO) and SHERPA calculations but overestimated by MG5_aMC NLO prediction. Since the predictions of inclusive Z + jets production at NLO order are in better agreement with data than that at LO. This could be an indication that the PDFs overestimate the b/c quarks content and can be useful to improve existing constraints on the b/c quarks content in the proton.

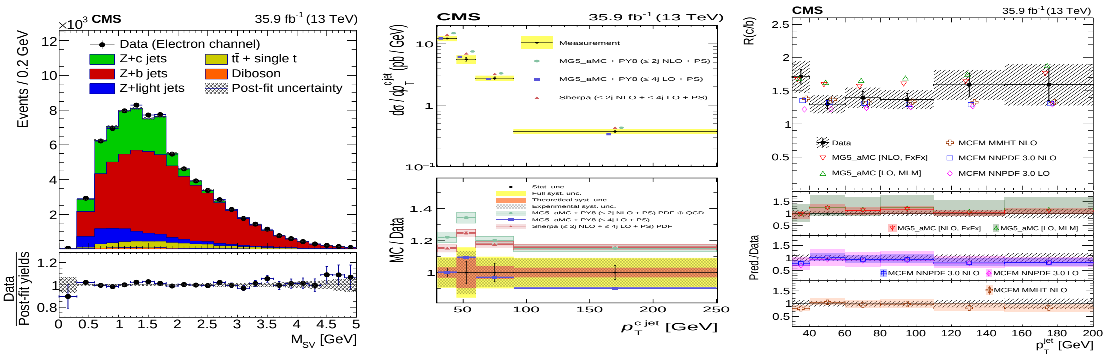

Figure 2: Secondary vertex invariant mass distributions derived from fits using the inclusive Z + HF jets data sample (left) [20]. Differential cross sections for inclusive Z + c jet production as a function of c jet p_T (middle) [19]. Measured, particle-level MG5_aMC, and parton-level MCFM cross section ratios R(c/b) as a function of jet p_T (right) [20].

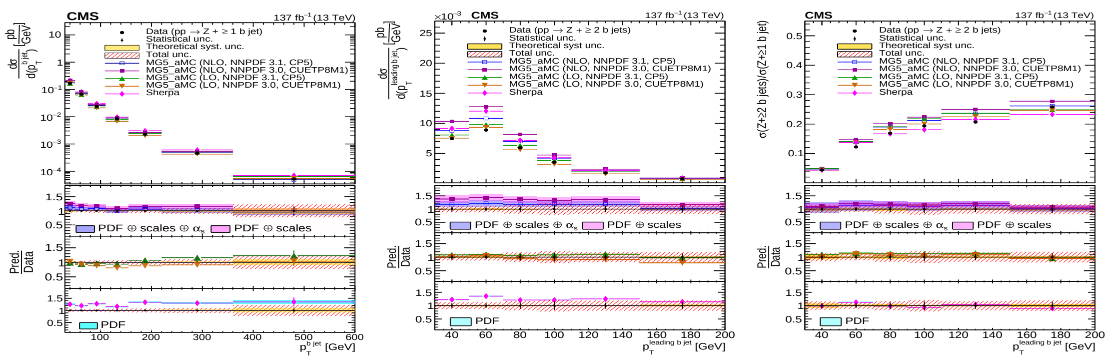

Figure 3: Differential cross section distribution for Z + ≥ 1 b jet (left) and Z + ≥ 2 b jets (middle) and cross section ratio of Z + ≥ 2 b jets to Z + ≥ 1 b jet as a function of leading b jet p_T [21].

4. Summary

The CMS experiments have a rich program of measurements related to heavy flavors and jets. Here, we presented an overview of recent measurements which are sensitive to different theoretical approaches and are used to probe the bottom, charm, and strange quark content of the proton. Present measurements can be used as input to further optimization of the simulation parameters.

References

[1] CMS Collaboration, *The CMS Experiment at the CERN LHC*, *JINST* **3** (2008) S08004

[2] CMS Collaboration, *Measurement of associated production of a W boson and a charm quark in proton-proton collisions at* $\sqrt{s}$ *= 13 TeV*, *Eur. Phys. J. C* **79** (2019)

[3] S. Alekhin, J. Blümlein, and S. Moch, *NLO PDFs from the ABMP16 fit*, *Eur. Phys. J. C* **78** (2018) 477

[4] ATLAS Collaboration, *Precision measurement and interpretation of inclusive* W^+, W^- *and* $Z/\gamma*$ *production cross sections with the ATLAS detector*, *Eur. Phys. J. C* **77** (2017) 367

[5] S. Dulat et al., *New parton distribution functions from a global analysis of quantum chromodynamics*, *Phys. Rev. D* **93** (2016) 033006

[6] L. A. Harland-Lang, A. D. Martin, P. Motylinski, and R. S. Thorne, *Parton distributions in the LHC era: MMHT 2014 PDFs*, *Eur. Phys. J. C* **75** (2015) 204.

[7] NNPDF Collaboration, *Parton distributions for the LHC run II*, *JHEP* **04** (2015) 040.

[8] NNPDF Collaboration, *Parton distributions from high-precision collider data*, *Eur.Phys. J. C* **77** (2017) 663.

[9] H1 and ZEUS Collaborations, *Combination of measurements of inclusive deep inelastic* $e^{\pm}p$ *scattering cross sections and QCD analysis of HERA data*, *Eur. Phys. J. C* **75** (2015) 580

[10] CMS Collaboration, *Measurement of associated W+charm production in pp collisions at* $\sqrt{s}$ *= 7 TeV*, *JHEP* **02** (2014) 013

[11] CMS Collaboration, *Measurement of the muon charge asymmetry in inclusive* $pp \to W + X$ *production at* $\sqrt{s} = 7$ *TeV and an improved determination of light parton distribution functions*, *Phys. Rev. D* **90** (2014) 032004.

[12] CMS Collaboration, *Measurement of the differential cross section and charge asymmetry for inclusive* $pp \to W^{\pm} + X$ *production at* $\sqrt{s} = 8$ *TeV*, *Eur. Phys. J. C* **76** (2016) 469.

[13] S. Alekhin et al., *HERAFitter*, *Eur. Phys. J. C* **75** (2015) 304.

[14] 2018. *xFitter web site*, `http://www.xfitter.org/xFitter`.

[15] NuTeV Collaboration, *Precise measurement of dimuon production cross-sections in muon neutrino Fe and muon anti-neutrino Fe deep inelastic scattering at the Tevatron*, *Phys. Rev. D* **64** (2001) 112006.

[16] CCFR Collaboration, *Determination of the strange quark content of the nucleon from a next-to-leading order QCD analysis of neutrino charm production*, *Z. Phys. C* **65** (1995) 189.

[17] NOMAD Collaboration, *A precision measurement of charm dimuon production in neutrino interactions from the NOMAD experiment*, *Nucl. Phys. B* **876** (2013) 339.

[18] A. Kayis-Topaksu et al., *Measurement of charm production in neutrino charged-current interactions*, *New J. Phys.* **13** (2011) 093002.

[19] CMS Collaboration, *Measurement of differential cross sections for Z bosons produced in association with charm jets in pp collisions at $\sqrt{s} = 13$ TeV*, *JHEP* **04** (2021)

[20] CMS Collaboration, *Measurement of the associated production of a Z boson with charm or bottom quark jets in proton-proton collisions at $\sqrt{s}$= 13 TeV*, *Phys. Rev. D* **102** (2020)

[21] CMS Collaboration, *Measurement of the production cross section for Z + b jets in proton-proton collisions at $\sqrt{s} = 13$ TeV*, *submitted to Phys. Rev. D*

[22] CMS Collaboration, *Identification of heavy-flavour jets with the CMS detector in pp collisions at 13 TeV*, *JINST* **13**, P05011 (2018).